Article ID: 1006-8775(2022) 02-0194-13

Spatiotemporal Variation of Water Vapor Budget over the Tibetan Plateau and Its Regulation on Precipitation

WANG Hui-mei (王慧美)[1, 2], ZHAO Ping (赵 平)[1, 2, 3]

(1. Collaborative Innovation Center on Forecast and Evaluation of Meteorological Disasters, Nanjing University of Information Science and Technology, Nanjing 210044 China; 2. State Key Laboratory of Severe Weather, Chinese Academy of Meteorological Sciences, Beijing 100081 China; 3. Institute of Tibetan Plateau & Polar Meteorology, Chinese Academy of Meteorological Sciences, Beijing 100081 China)

Abstract: The spatiotemporal variations of water vapor budget (Bt) and their relationships with local precipitation over the Tibetan Plateau (TP) are critical for understanding the characteristics of spatial distributions and evolutions of water resources over the TP. Based on a boundary of the TP, this paper explored the spatiotemporal characteristics of Bt over the TP using the European Centre for Medium-Range Weather Forecasts interim (ERA-Interim) reanalysis datasets. On the climatological mean, the TP is a water vapor sink throughout four seasons and the seasonal variation of Bt is closely associated with the water vapor budget at the southern boundary of the TP. The transient water vapor transport is quasi-meridional in the mid- and high-latitude areas and plays a leading role in winter Bt but contributes little in other seasons. At the interannual timescale, the variation of Bt is mainly determined by anomalous water vapor transports at the western and southern boundaries. The Bay of Bengal, the North Arabian Sea, and mid-latitude West Asia are the main sources of excessive water vapor for a wetter TP. At the southern and western boundaries, the transient water vapor budget regulates one-third to four-fifths of Bt anomalies. Moreover, the variability of the TP Bt is closely associated with precipitation over the central-southern and southeastern parts of the TP in summer and winter, which is attributed to the combined effect of the stationary and transient water vapor budgets. Given the role of the transient water vapor transport, the linkage between the TP Bt and local precipitation is tighter.

Key words: Tibetan Plateau; water vapor budget; transient water vapor transport; stationary water vapor transport; precipitation

CLC number: P466 **Document code:** A

Citation: WANG Hui-mei, ZHAO Ping. Spatiotemporal Variation of Water Vapor Budget over the Tibetan Plateau and Its Regulation on Precipitation [J]. Journal of Tropical Meteorology, 2022, 28(2): 194-206, https://doi.org/10.46267/j.1006-8775.2022.015

1 INTRODUCTION

The Tibetan Plateau (TP) is the highest and largest plateau in the world, with an area of 2.5 million km^2 and an average elevation over 4000 meters. The TP is also recognized as the "Asian water tower" due to abundant water resources stored as glaciers, lakes, and rivers (Yao et al. [1]; Xu et al. [2]; Ma et al. [3]). Seasonal melting of snowpacks and glaciers provides water for several major rivers in Asia, such as the Indus River, the Yarlung Zangbo River, the Yangtze River, and the Yellow River, modulating adjacent ecosystems and feeding more than two billion people (Immerzeel et al. [4]; Yao et al. [5]). Because of the thermodynamic effect of the TP, water vapor can be continuously induced from surrounding oceans or lands to the TP (Xu et al. [2]; Zhao et al. [6]; Zhou et al. [7]) and then forms precipitation and supplies water resources over the TP. Therefore, investigating the variation of water vapor budget and its relationship with the regional precipitation over the TP is critical for understanding the characteristics of spatial distribution and evolution of water resources over the TP.

Regional water vapor budget depends on water vapor transport conditions. Numerous studies have investigated the climatological characteristics of water vapor sources and transport pathways of the TP, especially in summer. It is found that external water vapor transportation and local surface evapotranspiration govern water vapor sources of the TP (Ye and Gao [8]; Yao et al. [9]; Curio et al. [10]; Wang et al. [11]; Zhang et al. [12]). External water vapor transportation can be roughly clarified into four channels for the TP and its surrounding area: the mid-latitude westerly belt channel, the Bay of Bengal-Brahmaputra channel, the Arabian Sea-Indian peninsula channel, and the western Pacific-South China Sea channel (Yao et al. [9]; Sugimoto et

Submitted 2021-11-25; **Revised** 2022-02-15; **Accepted** 2022-05-15

Funding: Second Scientific Expedition on the Qinghai-Tibet Plateau (2019QZKK020803); Strategic Priority Research Program of Chinese Academy of Sciences Pan-Third Pole Environment Study for a Green Silk Road (XDA2010030807)

Biography: WANG Hui-mei, Ph. D. candidate, primarily undertaking research on climate over the Tibetan Plateau.

Corresponding author: ZHAO Ping, e-mail: zhaop@cma.gov.cn

al. [13]; Shi and Shi [14]; Bothe et al. [15]; Gao et al. [16]; Zhou et al. [17]; Feng and Zhou [18]). In summer, the westerly flows southward along the west edge of the TP, turns eastward around 28 °N, merges with the southwesterly from the Indian Ocean, and eventually enters the southwestern TP (Feng and Zhou [18]; Meng et al. [19]). Several studies indicated that the southern boundary is the main channel for water vapor supply of the TP in summer and water vapor transportation via the western boundary reaches up to 30%–45% of that via the southern boundary (Feng and Zhou [18]; Gao et al. [20]). Summer water vapor budget (Bt) over the TP is larger than that in the other three seasons and decreases from the southeast to the northwest of the TP (Meng et al. [19]; Xu et al. [21]; Zhou et al. [22]).

Anomalous water vapor transport is closely connected with regional atmospheric circulation. From the perspective of influencing precipitation over the TP, many scholars have studied the corresponding anomalous circulation and water vapor transport anomalies (Wang et al. [11]; Zhang et al. [12]; Feng and Zhou [18]; Liu and Yin [23]; Gao et al. [24]; Dong et al. [25]; Jiang et al. [26]; Chen et al. [27]; Yan et al. [28]; Liu et al. [29]; Liu et al. [30]; Hu et al. [31]). More-than-normal precipitation in summer over the southeastern TP is associated with an anomalous anticyclonic water vapor transport over the northern India and the Bay of Bengal (Feng and Zhou [18]; Jiang et al. [26]). Jiang et al. [26] pointed out that the positive sea surface temperature (SST) anomalies in the Indian Ocean could excite the abovementioned anomalous anticyclone. Wang et al. [11] found that the summer North Atlantic Oscillation (NAO) could weaken water vapor transportation at the western boundary of the TP. At the interdecadal timescale, Liu et al. [30] demonstrated that the anomalous water vapor budget over the northern TP is jointly regulated by the Atlantic Multidecadal Oscillation (AMO) and the Interdecadal Pacific Oscillation (IPO). Numerous evidence also showed a wetting trend over the TP, but the trend is spatially inhomogeneous (Zhang et al. [12]; Zhou et al. [22]; Yan [28]; Xie et al. [32]; Lu et al. [33]; Lu et al. [34]). Specifically, Xie et al. [32] examined summer atmospheric water vapor in five sub-regions of the TP and found that summer Bt has obviously increasing (decreasing) trends in the northeastern (central-northern and central-southern) TP from 1979 to 2010. Zhou et al. [22] focused on Bt over the entire TP and confirmed that the summer TP has undergone a transition from dry to wet phase in the middle of the 1990s due to a significant decrease in the water vapor export at the eastern boundary of the TP.

The abovementioned results are usually based on monthly mean datasets, which ignores shorter timescale variations. The monthly mean vertical integral of the water vapor flux can be decomposed into the stationary and transient components. The stationary water vapor transport is defined as the transportation by monthly mean circulation systems, such as planetary wind belts, the cross-equatorial jet, and subtropical highs (Yi and Tao [35]; Zhou et al. [36]). Liu and Cui [37] pointed out that the transient water vapor transport is primarily associated with disturbances, such as enclosed cyclone (anticyclone) systems and moving troughs (ridges). Piao et al. [38] confirmed that for the annual cycle, the transient water vapor transport has an important influence on the net water vapor supply over Siberia and Northeast Asia, but the contribution of the transient water vapor transport is very limited at the interannual timescale. Generally, the magnitude of the transient water vapor flux is one order smaller than that of the stationary and total water vapor fluxes. Therefore, total water vapor flux is usually substituted by the stationary water vapor flux when the processes of water vapor transport are examined although one may wonder whether such a replacement will cause non-negligible discrepancies at different timescales. The present study attempts to examine the contribution of the transient and stationary water vapor transports to Bt over the TP at climate mean and interannual timescales, which may help us systematically understand the variability of the TP Bt.

2 DATA AND METHODS

This study focuses on the TP area (26°–40°N, 70°–104° E) with the altitude above 2000 m (i. e., the area enclosed by polygonal lines in Fig. 1). The European Centre for Medium-Range Weather Forecasts interim (ERA-Interim) reanalysis datasets with the horizontal resolutions of 1.5° × 1.5° and 0.25° × 0.25° are used, including monthly and 6-hourly surface pressure, specific humidity, and horizontal winds (Dee et al. [39]). Gao et al [16] pointed out that the ERA-Interim dataset performs better than other reanalysis datasets in water vapor budget around the TP. Daily precipitation at 122 meteorological stations (black dots in Fig. 1) in the TP area is provided by the China Meteorological Administration (CMA). Daily gridded precipitation is also applied from Asian Precipitation–Highly Resolved Observational Data Integration toward Evaluation of Water Resources (APHRODITE) with the horizontal resolutions of 0.25° × 0.25° (Yatagai et al. [40]), spanning from 1951 to 2015. Monthly mean precipitation is provided by the University of East Anglia Climatic Research Unit (CRU) with the horizontal resolutions of 0.5° × 0.5° (Harris et al. [41]). Except for the APHRODITE precipitation, the above data are all extracted from 1979 to 2018.

The vertically integrated water vapor flux (Q) and Bt are calculated as follows, respectively.

$$Q = -\frac{1}{g}\int_{p_s}^{p_t} q\mathbf{V}\mathrm{d}p \tag{1}$$

$$\mathrm{Bt} = \oint Q\mathrm{d}l = \mathrm{Bw} + \mathrm{Be} + \mathrm{Bs} + \mathrm{Bn} \tag{2}$$

where g is the gravity acceleration; p_s is the surface pressure; q is the specific humidity; $\mathbf{V}$ is the horizontal

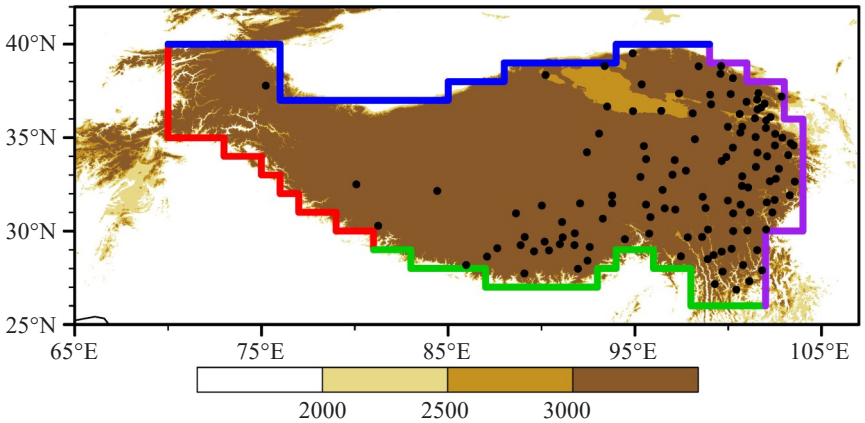

Figure 1. The boundary (elevation greater than 2000 m) and 122 stations (black dots) of the Tibetan Plateau (TP), in which western, southern, eastern, and northern boundaries are denoted in red, green, purple, and blue, respectively.

wind vector; p_t is the pressure of top layer, which is equal to 300 hPa (water vapor above 300 hPa is neglected) in formula (1). l in formula (2) is the boundary curve of the TP. Bt over the TP area enclosed by the curve l is the sum of water vapor budget at four boundaries: the western (Bw), southern (Bs), eastern (Be), and northern (Bn) boundaries. Compared with the regional mean of precipitable water or water vapor convergence, it seems to be more reasonable to measure the TP BT through calculating Bs, Bn, Bw, and Be, by measuring the net atmospheric water vapor amounts, since there are more observed data assimilated into the atmospheric reanalysis datasets in the adjacent areas of the TP in contrast to the inner TP (Zhou et al. [22]).

According to Piao et al. [38], the monthly total water vapor flux can be decomposed as the stationary and transient components and is calculated as follows:

$$Q = -\frac{1}{g}\int_{p_s}^{p_t} \bar{\mathbf{V}}\bar{q}\,\mathrm{d}p - \frac{1}{g}\int_{p_s}^{p_t} \overline{\mathbf{V}'q'}\,\mathrm{d}p = Q1 + Q2 \quad (3)$$

where Q is the monthly vertical water vapor flux. The two terms on the right side stand for the stationary water vapor flux ($Q1$) related to mean wind and the transient water vapor flux ($Q2$) related to transient wind, respectively. That is, the sum of $Q1$ and $Q2$ is the total water vapor flux (Q). The overbar denotes the monthly average, and the prime is a transient deviation from the mean. Accordingly, Bt is the sum of the stationary water vapor budget (Bt1) and the transient term (Bt2). To quantitatively estimate the contribution of the transient water vapor transport to the TP Bt, the contribution rate of the transient water vapor transport (Rate) is defined as follows:

$$\mathrm{Rate} = \frac{\mathrm{Bt2}}{\mathrm{Bt}} \times 100\% \quad (4)$$

Correlation, composite, and empirical orthogonal function (EOF) methods are used in this study. Unless otherwise stated, the statistical significance tests are performed using the two-tailed Student's t-test. Spring, summer, autumn, and winter seasons are March-May, June-August, September-November, and December-February, respectively.

3 CLIMATOLOGY AND ANNUAL CYCLE OF THE TP WATER VAPOR BUDGET

Figure 2 presents climatological mean water vapor transport. In spring and winter, the TP, even the whole Eurasian continent, is under the control of the approximately westerly-induced water vapor transport (Figs. 2a and 2d). Summer water vapor transport around the TP shows more complex characteristics and is associated with the mid-latitude westerly and the Indian summer monsoon (Fig. 2b). Similar to the conclusions in Feng and Zhou [18], the westerly and strong southwesterly flows are divided into two when they encounter the barrier of the TP. The Yarlung Zangbo River valley which is in the west-east direction over the southern TP and several meridionally oriented valleys, such as the Nujiang River and Lancang River valleys, would facilitate the transport of water vapor into the inner TP (Xu et al. [2]; Gao et al. [20]). In autumn, apart from the Bay of Bengal (Fig. 2c), water vapor transport from the South China Sea also contributes to the water vapor budget (Bt) over the TP, which is more evident in the lower troposphere (figure omitted).

Figure 3 shows water vapor amount transported into the TP via each boundary in four seasons. Water vapor flows into the TP through the western and southern boundaries and flows into the downstream areas through the eastern boundary in the whole year. Water vapor budget at the northern boundary (Bn) is very small. Water vapor budgets at the western (Bw) and eastern (Be) boundaries counteract each other throughout the year. Water vapor budget at the southern boundary (Bs) varies largely, from 25×10^6 kg s^{-1} (in winter) to 88×10^6 kg s^{-1} (in summer), which would directly influence the amount of water vapor budget (Bt) over the TP. Note that Bs is possibly overestimated by an usual rectangle boundary, especially in the eastern TP. According to our estimation, summer Bs at the rectilinear boundary in Feng and Zhou [18] and Zhou et

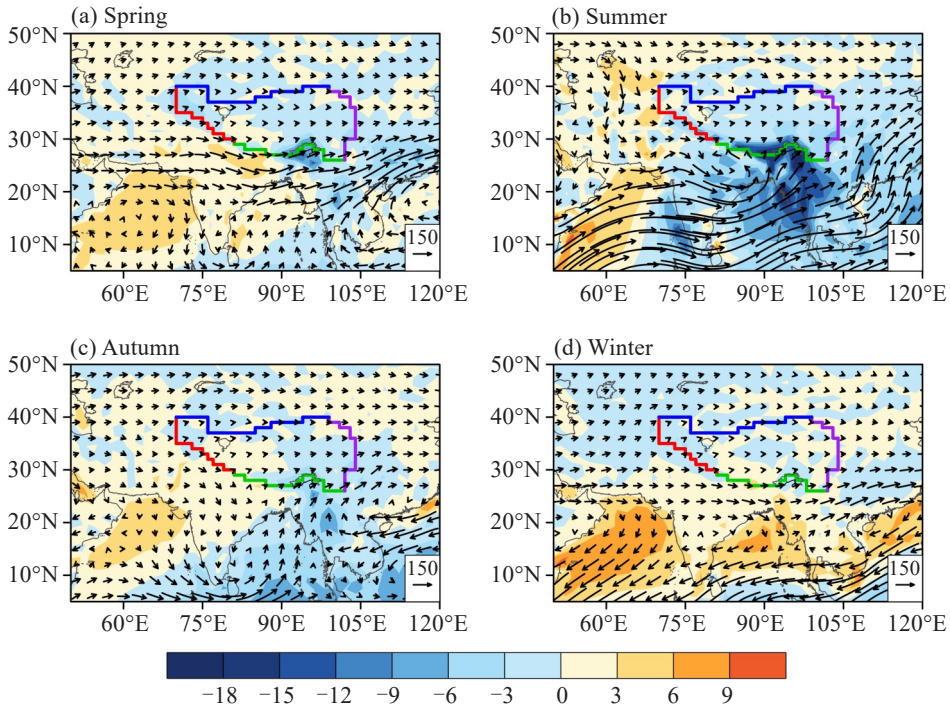

Figure 2. Vertically integrated water vapor flux (vectors; units: kg m^{-1} s^{-1}) and divergence (shaded; units: 10^{-5} kg m^{-2} s^{-1}) in (a) spring, (b) summer, (c) autumn, and (d) winter.

al. [22] (from 81°E to 98°E) are larger by at least 30 × 10^6 kg s^{-1} compared with our zigzag boundary. Thus, a more elaborative definition of the TP boundary is important to reasonably estimate Bt over the TP. According to Table 1, as the "water tower of Asia", the entire TP is a huge water vapor sink in four seasons, in which net water vapor income in summer is the largest (86.57 × 10^6 kg s^{-1}), accounting for 57.5% of the net water vapor input in the whole year. This is also seen from the noticeable water vapor convergences over the TP in Fig. 2b. Then spring (autumn) Bt is about 39.42 × 10^6 kg s^{-1} (15.15 × 10^6 kg s^{-1}). Although winter Bt is the smallest, below 10 × 10^6 kg s^{-1}, it is still the key factor of winter precipitation.

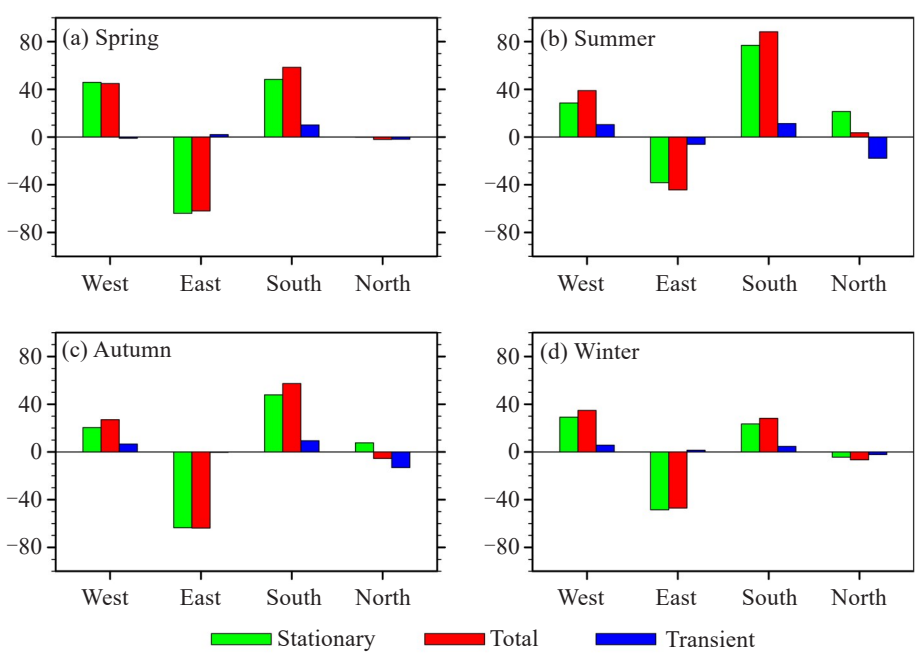

Figure 3. Climatological water vapor budget (units: 10^6 kg s^{-1}) over the TP at four boundaries in (a) spring, (b) summer, (c) autumn, and (d) winter. The red bars denote the total water vapor budget (Bt), and green and blue bars denote the stationary (Bt1) and transient (Bt2) water vapor budgets, respectively.

Table 1. Climatology of the total (Bt), stationary (Bt1), and transient (Bt2) water vapor budget over the TP in four seasons (units: 10^6 kg s^{-1}). Rate is the contribution rate of the transient water vapor transport to Bt (units: %).

	Spring	Summer	Autumn	Winter
Bt	39.40	86.57	15.15	9.37
Bt1	30.02	88.70	12.50	−0.2
Bt2	9.38	−2.13	2.65	9.64
Rate	23.8	−2.5	17.5	102.9

The monthly mean water vapor flux and budget can be decomposed into two terms based on Eq. (3): the stationary and transient parts. The spatial distribution and magnitude of $Q1$ (figure omitted) are generally similar to those of Q (Fig. 2). The spatial distribution of the transient term is displayed in Fig. 4. The transient water vapor transport is quasi-meridional in the mid- and high-latitude Asia during four seasons, which is consistent with the result of Wang et al. [42]. Although $Q2$ is much smaller than Q and $Q1$, the transient water vapor transportation could deliver warm and wet air from the low-latitude areas to the TP or convey water vapor over the TP northward via the northern boundary, causing obvious water vapor divergence (convergence) in summer (winter) over the TP (Figs. 4b and 4d). Comparisons between the stationary water vapor budget (Bt1, green bars) and the transient term (Bt2, blue bars) with the total Bt (red bars) at four boundaries (Fig. 3) show that Bt1 is close to Bt at the western, eastern, and southern boundaries, which suggests that the stationary water vapor transport generally dominates the total Bt. At the northern boundary, Bt1 and Bt2 cancel out each other in summer and autumn, thus resulting in a small Bt. For the whole TP, the winter Bt is almost entirely contributed by the transient water vapor budget relative to the stationary term, with a high contribution rate of 103%. The transient water vapor transport controls nearly one-fifth of the TP Bt in spring and autumn. On the climatological mean, Bt2 could be neglected in summer.

4 INTERANNUAL VARIATION OF WATER VAPOR BUDGET AND ITS RELATIONSHIP WITH PRECIPITATION OVER THE TP

Previous studies suggested that summer precipitation over the southeastern TP is associated with anomalous anticyclonic water vapor transport over the northern India and the Bay of Bengal (Feng and Zhou [18]; Jiang et al. [26]). The interannual variability of winter precipitation over the western TP is linked to the anomalous southwesterly water vapor transport to the south of this region (Liu et al. [29]). However, these results mainly focused on sub-regions and used monthly mean datasets. In this section, we consider the TP as a whole, discuss the variation of the TP Bt during four

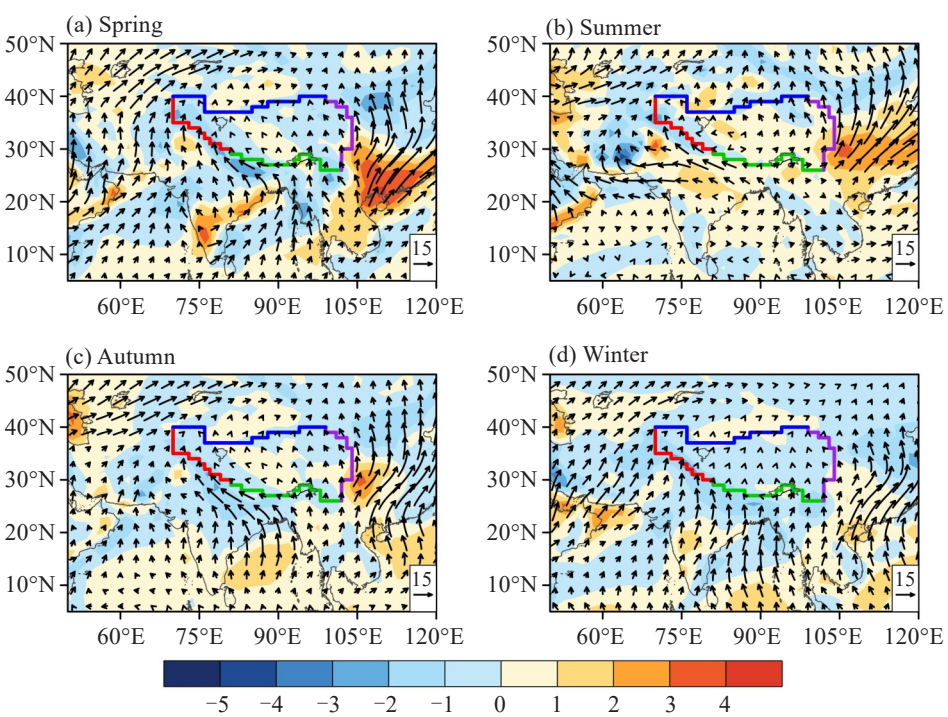

Figure 4. The same as Fig. 2, but for the transient water vapor flux.

seasons, examine the contributions of the stationary and transient water vapor transports to Bt, and investigate their relationship with the precipitation over the TP at the interannual timescale.

4.1 *Interannual variability of water vapor budget*

Figure 5 presents the time series of seasonal mean Bt (black solid line), Bt1 (red line with dots), and Bt2 (blue line with dots) over the TP during 1979−2018. The Bt over the TP shows a significantly increasing trend in spring, summer, and autumn, with the trend of 2.9×10^5 kg s^{-1} yr^{-1}, 5.6×10^5 kg s^{-1} yr^{-1} and 1.1×10^5 kg s^{-1} yr^{-1}, respectively. Meanwhile, the summer Bt, with the largest wetting trend, experienced a significant mutation around 1994, which is in accordance with the study of Zhou et al. [22]. Bt2 significantly increases only in spring. In summer and autumn, Bt1 dominates the wetting process. Bt also exhibits obvious interannual variations after removing the linear trends during four seasons (figure omitted). Based on the standard time series of Bt after removing the linear trends (figure omitted), the six highest and lowest years beyond 0.9 and −0.9 standard deviation of BT are selected during every season (shown in Table 2). We further compare water vapor transport in wet and dry years (Fig. 6).

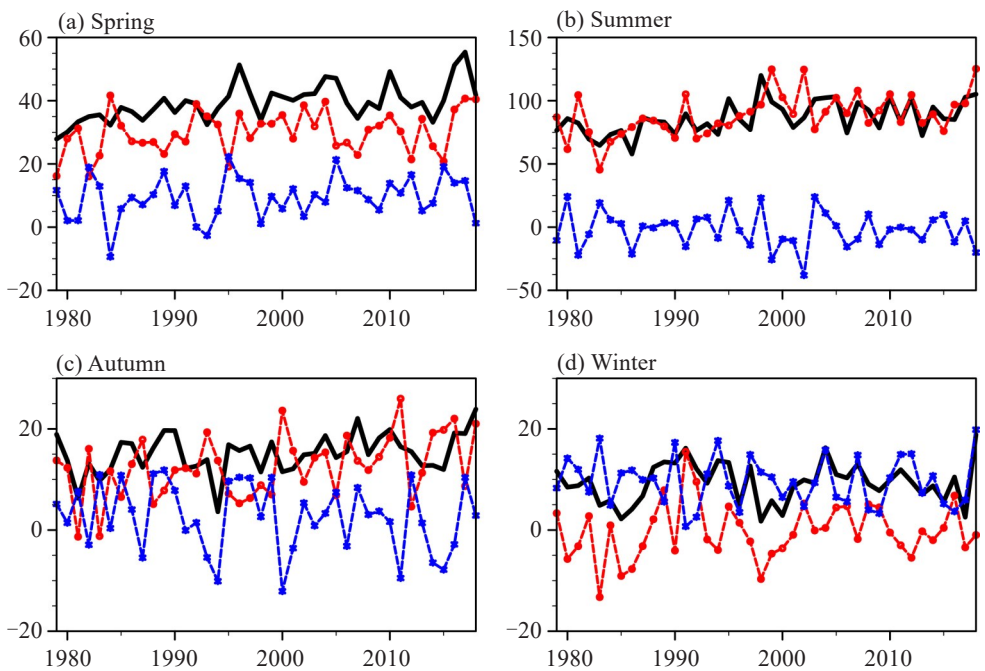

Figure 5. Time series of Bt (black solid line), Bt1 (red line with red dots), and Bt2 (blue line with blue dots) over the TP during 1979−2018 in (a) spring, (b) summer, (c) autumn, and (d) winter (units: 10^6 kg s^{-1}).

Table 2. Wet and dry years for each season over the TP.

	Wet years	Dry years
Spring	1996, 2004, 2005, 2010, 2016, 2017	1979, 1993, 1998, 2007, 2012, 2014
Summer	1995, 1998, 1999, 2003, 2004, 2005	1983, 1986, 1994, 2006, 2009, 2013
Autumn	1979, 1989, 1990, 2007, 2010, 2018	1981, 1994, 1998, 2013, 2014, 2015
Winter	1989, 1990, 1991, 1994, 2004, 2018	1985, 1986, 1996, 1998, 2000, 2017

In spring (Fig. 6a), anomalous water vapor convergence appears over most of the TP and excessive water vapor generally comes from the southwesterly-induced water vapor transportation from the Bay of Bengal. The anomalous westerly-induced water vapor transportation on the southern side of the TP (85°E−95°E) also contributes to anomalous water vapor convergences around the Grand Canyon of the Yarlung Zangbo River, which may be related to the active trough to the south of TP in spring (Li et al. [43]). In summer, water vapor convergence anomalies strengthen remarkably and the evident signals are distributed in the central-southern and the southeasten parts of the TP and its southern side region, even more than -6×10^{-5} kg m^{-2} s^{-1}. This arises from the intensified water vapor transportation from the northern Arabian Sea and the north side of the Bay of Bengal. In autumn, the extra water vapor from the Bay of Bengal and the South China Sea is transported into the southeastern TP and contributes to the local water vapor convergence. In winter, the southwesterly-induced water vapor transport from the Arabian Peninsula to the western side of the TP

also remarkably strengthens. Abundant water vapor flows into the western TP where strong water vapor convergence is identified. Apart from that, the southeastern TP also gains more-than-normal water vapor for a larger Bt in winter. Table 3 further gives the quantitative differences of four boundaries between wet and dry years of Bt. The results show that the differences of Bs are larger than the ones at other boundaries in spring, summer, and autumn when the TP is wetter. In winter, the difference of Bw is more significant than that of Bs and contributes to a wetter TP. This means that the yearly variation of Bt is primarily regulated by anomalous water vapor supplies at the western and southern boundaries and Bs plays a more vital role in all reasons except for winter. We can also see that the difference of Be between wet and dry years is generally negative, which indicates that water vapor exports from the eastern boundary increase when the TP is wetter.

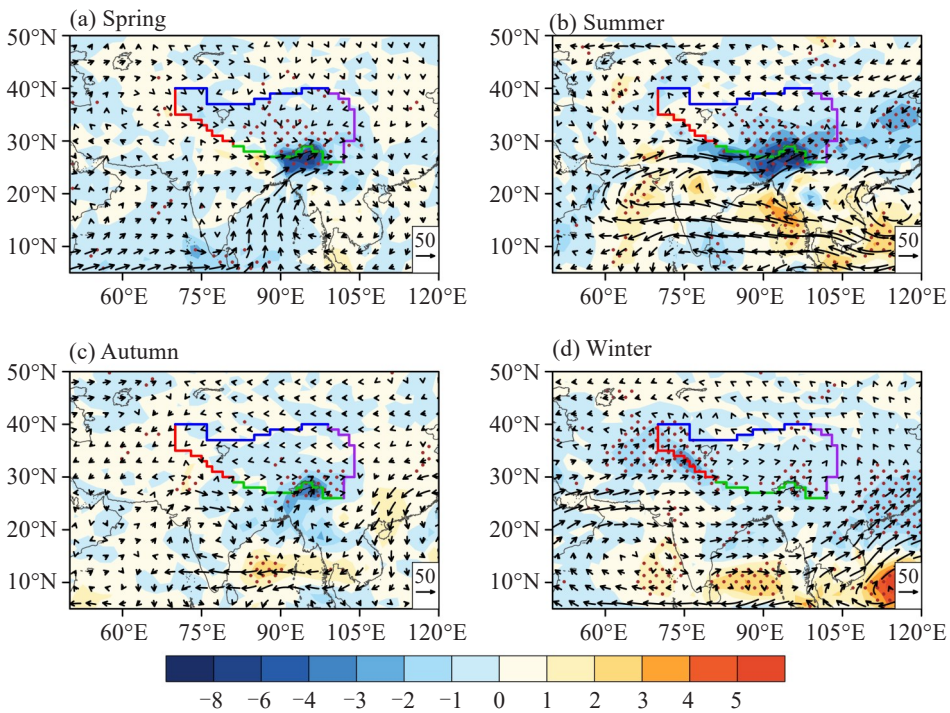

Figure 6. Composite differences (wet minus dry years) of the total water vapor flux (vector; units: kg m^{-1} s^{-1}) and its divergence (shaded; units: 10^{-5} kg m^{-2} s^{-1}) in (a) spring, (b) summer, (c) autumn, and (d) winter. Red dotted areas denote the differences of water vapor flux divergence significant at the 90% confidence level.

Table 3. The total (Bt), stationary (Bt1), and transient (Bt2) water vapor budgets in four seasons at the western boundary (Bw), eastern boundary (Be), southern boundary (Bs), and northern boundary (Bn) during wet and dry years and their differences (units: 10^6 kg s^{-1}).

		Bw			Be			Bs			Bn		
		wet	dry	diff	wet	dry	diff	wet	dry	diff	wet	dry	diff
Spring	Bt1	50.3	44.7	5.6	−68.1	−64.8	−3.3	53.0	45.9	**7.1***	0.5	−0.3	0.8
	Bt2	−0.9	0.8	−1.7	2.9	2.7	0.2	12.7	7.5	**5.2***	−0.2	−3.4	3.2
	Bt	49.4	45.5	3.9	−65.2	−62.1	−3.1	65.7	53.4	**12.3***	0.3	−3.7	4.0
Summer	Bt1	32.6	25.1	**7.5***	−40.1	−39.6	−0.5	82.6	71.9	**10.7***	20.4	21.2	−0.8
	Bt2	9.2	11.3	−2.1	−5.9	−5.6	−0.3	23.5	0.2	**23.3***	−17.8	−14.3	−3.5
	Bt	41.8	36.4	**5.4***	−46.0	−45.2	−0.8	106.1	72.1	**34.0***	2.6	6.9	−4.3
Autumn	Bt1	17.6	19.3	−1.7	−61.8	−62.7	0.9	50.4	46.9	**3.5***	8.2	8.4	−0.2
	Bt2	7.0	9.0	−2.0	−0.7	−1.2	0.5	11.9	4.5	**7.4***	−12.1	−14.5	2.4
	Bt	24.6	28.3	−3.7	−62.5	−63.9	1.4	62.3	51.4	**10.9***	−3.9	−6.1	2.2
Winter	Bt1	31.3	25.6	**5.7***	−49.8	−48.7	−1.1	25.7	22.1	3.6	−4.8	−4.3	−0.5
	Bt2	8.5	3.8	**4.7***	1.0	2.0	**−1.0+**	6.8	3.3	3.5	−3.5	−0.7	**2.8***
	Bt	39.8	29.4	**10.4***	−48.8	−46.7	−2.1	32.5	25.4	7.1	−8.3	−5.0	**−3.3***

Note: the differences indicated by an asterisk (*) are significant at the 90% confidence level.

The effects of the stationary and transient water vapor transports on the interannual variations of Bt are also examined. Water vapor circulation of the stationary term is similar to the total water vapor transportation on the whole, which suggests that the mean flow could basically represent the anomalous water vapor circulation pattern over and around the TP (Figs. 7a−7d). Despite the smaller magnitude of the transient water vapor transportation, it affects water vapor supply at the western boundary of the TP in winter (Fig. 7h). From Table 3, we can also see that at the southern and western boundaries, which are the key factors influencing the interannual variability of the TP Bt, the transient water vapor transport could modulate the change of the TP Bt. The contribution rate of the transient term to Bt is 41%, 51%, 77%, and 36% in spring, summer, autumn, and winter, respectively. Noted that the stationary water vapor transport on the southern side of the TP substantially intensifies in Fig. 7b, yet the difference of Bt1 at the southern boundary is smaller than that of Bt2 in summer. This is due to an opposite effect of anomalous water vapor transportation by the meridional mean flow between the east and west parts of the southern boundary where increased water vapor inflow and outflow occur, respectively. In short, we conclude that the stationary and transient water vapor transports jointly adjust Bt over the TP at the interannual timescale in four seasons, in which the transient term contributes to 1/3–4/5 of Bt anomalies.

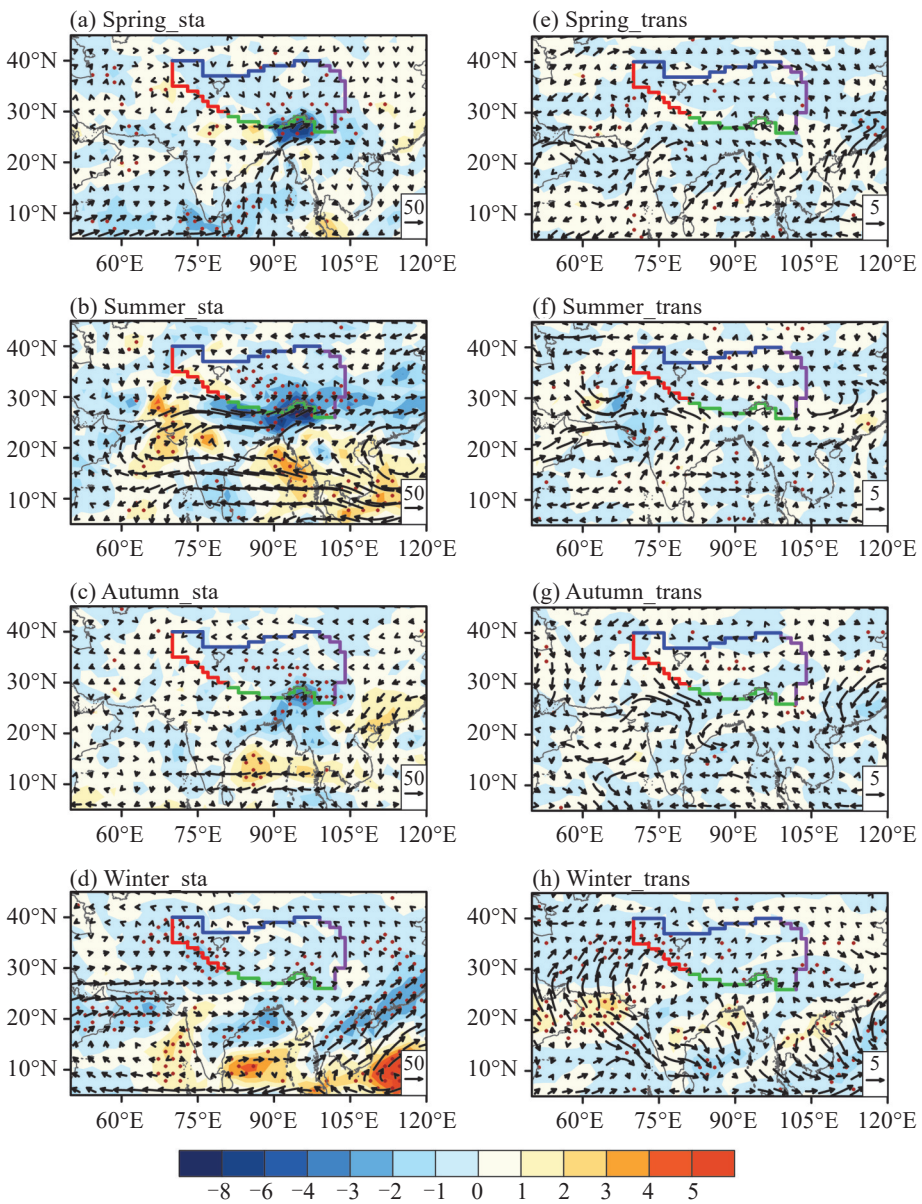

Figure 7. Composite differences (wet minus dry years) of the stationary water vapor flux (vector; units: kg m^{-1} s^{-1}) and its divergence (shaded; units: 10^{-5} kg m^{-2} s^{-1}) in (a) spring, (b) summer, (c) autumn and (d) winter. (e)−(h) as in (a)−(d), but for the transient term. Red dotted areas denote the differences of water vapor flux divergence significant at the 90% confidence level.

4.2 *The relationship between water vapor budget and precipitation over the TP*

Water vapor budget influences the local precipitation. Fig. 8 shows the spatial distribution of correlation coefficients of Bt, Bt1, and Bt2 with precipitation during 1979–2018. In spring and autumn (Figs. 8a and 8c), although a positive correlation covers most of the TP, significant signals only appear around the Yarlung Zangbo River valley, and this is primarily attributed to anomalous water vapor transport from the Bay of Bengal (Figs. 6a and 6c). In summer and winter (Figs. 8b and 8d), Bt has a close linkage with precipitation over the central-southern and southeastern parts of the TP (black boxes in Fig. 8; CSETP hereafter; 87° – 102° E, 28° – 34° N), with correlation coefficients above 0.4. That is, more precipitation would occur over this region when Bt is larger. It is also found that Bt1 and Bt2, with a smaller magnitude, both have an impact on the CSETP precipitation in different domains (Figs. 8f, 8h, 8j, and 8l). The correlation maps of Bt, Bt1, and Bt2 based on the CRU and APHRODITE precipitation datasets also show a similar pattern (Fig. 9): the anomalous water vapor budgets caused by the stationary circulation and frequent disturbance could effectively regulate precipitation over the TP. When combining the effect of the two components, the significantly correlated areas expand remarkably, and the TP Bt matches better with precipitation. This also indicates that the linkage between precipitation and water vapor budget utilized by monthly mean datasets may be underestimated in the previous studies.

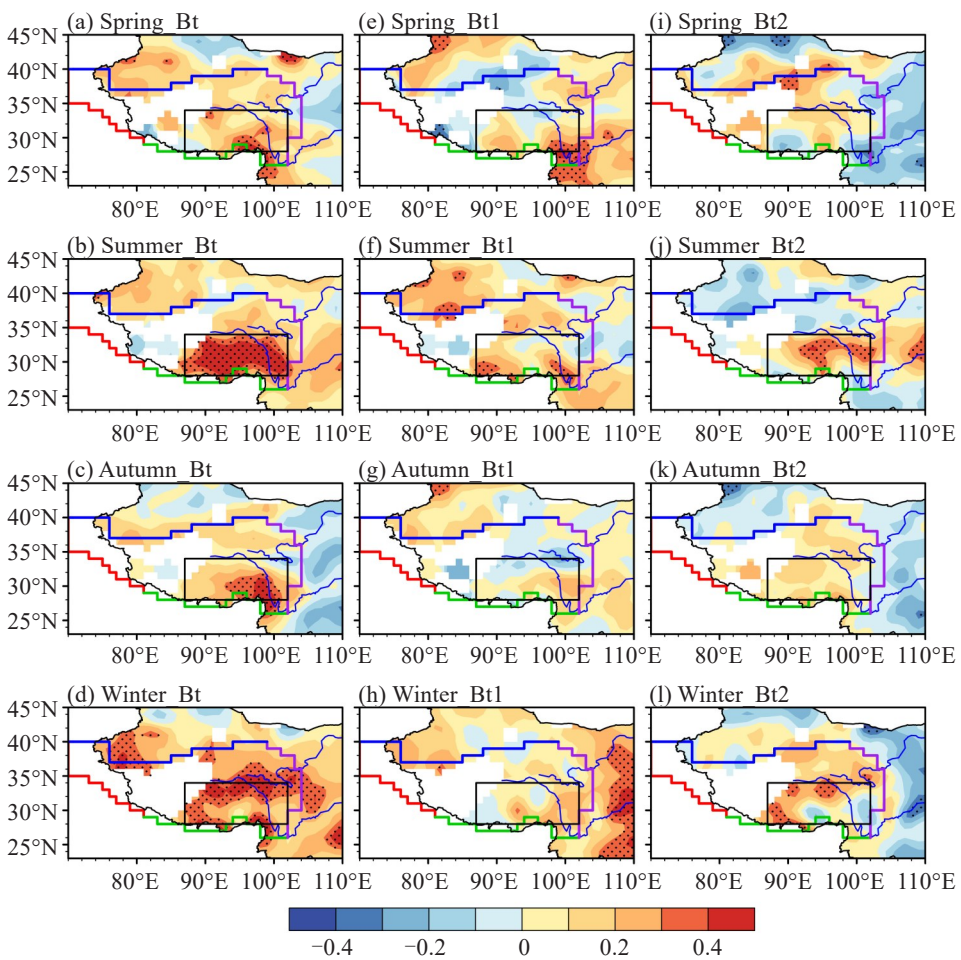

Figure 8. Spatial distribution of correlation coefficients between the total water vapor budget (Bt) and precipitation in (a) spring, (b) summer, (c) autumn, and (d) winter. (e)–(h) as in (a)–(d), but for the stationary water vapor budget (Bt1). (i)–(j) as in (a)–(d), but for the transient water vapor budget (Bt12). The dotted areas denote the correlation significant at the 90% confidence level. The linear trends of water vapor budget and precipitation have been removed. The black rectangle box denotes the CSETP region.

An EOF analysis is performed on the detrended summer and winter precipitation based on observational data. The results indicate that precipitation generally exhibits a nearly consistent variation over the CSETP region (figure omitted). This has also been confirmed based on other gridded datasets in previous studies (Jiang et al. [26]; Hu et al. [31]; Jiang et al. [44]). Then CSETP precipitation index is constructed by calculating a regional average precipitation over the CSETP. Table 4 summarizes the correlation coefficients of the CSETP precipitation index with Bt, Bt1, and Bt2 in summer and winter. The results show that the CSETP precipitation is

highly correlated with Bt, with correlation coefficients above 0.65. The correlation coefficients of Bt1 and Bt2 are smaller than that of Bt, with their correlation coefficients below 0.4. Clearly, the correlation coefficients between Bt and the CSETP precipitation index become higher after taking Bt2 into account. This result is in accordance with that in Fig. 7. That is, using monthly mean datasets, indicating the stationary water vapor transport, possibly underestimates the linkage between the TP Bt and precipitation over the southeastern TP in summer and winter. Thus, it is appropriate and necessary to consider the transient water vapor transport when exploring the impacts of Bt on precipitation over the TP.

Besides, the TP Bt anomalies are also be related to precipitation over India and eastern China in Fig. 9. Nevertheless, there are differences between the highly relevant areas associated with Bt and Bt1. For example, the correlation maps of summer Bt (Figs. 9a and 9g) could better reflect the dipole pattern of precipitation anomalies between the eastern TP and the middle-northwestern India, which is the first mode of summer precipitation at the interannual timescale and should be considered as an interactive system (Jiang et al. [26]). However, Bt1 could not depict this seesaw phenomenon. Furthermore, the TP Bt affects anomalous precipitation over the Yangtze-Huaihe valley (Figs. 9a and 9g). Several studies pointed out that the Tibetan Plateau vortex has a positive correlation with anomalous precipitation in this region (Hu et al. [45]; Zhao et al. [46]). However, the key area of anomalous precipitation associated with Bt1 is located in South China (Figs. 9b and 9h). Therefore, when illustrating the relationship between water vapor of the TP and precipitation anomalies, Bt is more appropriate compared to Bt1.

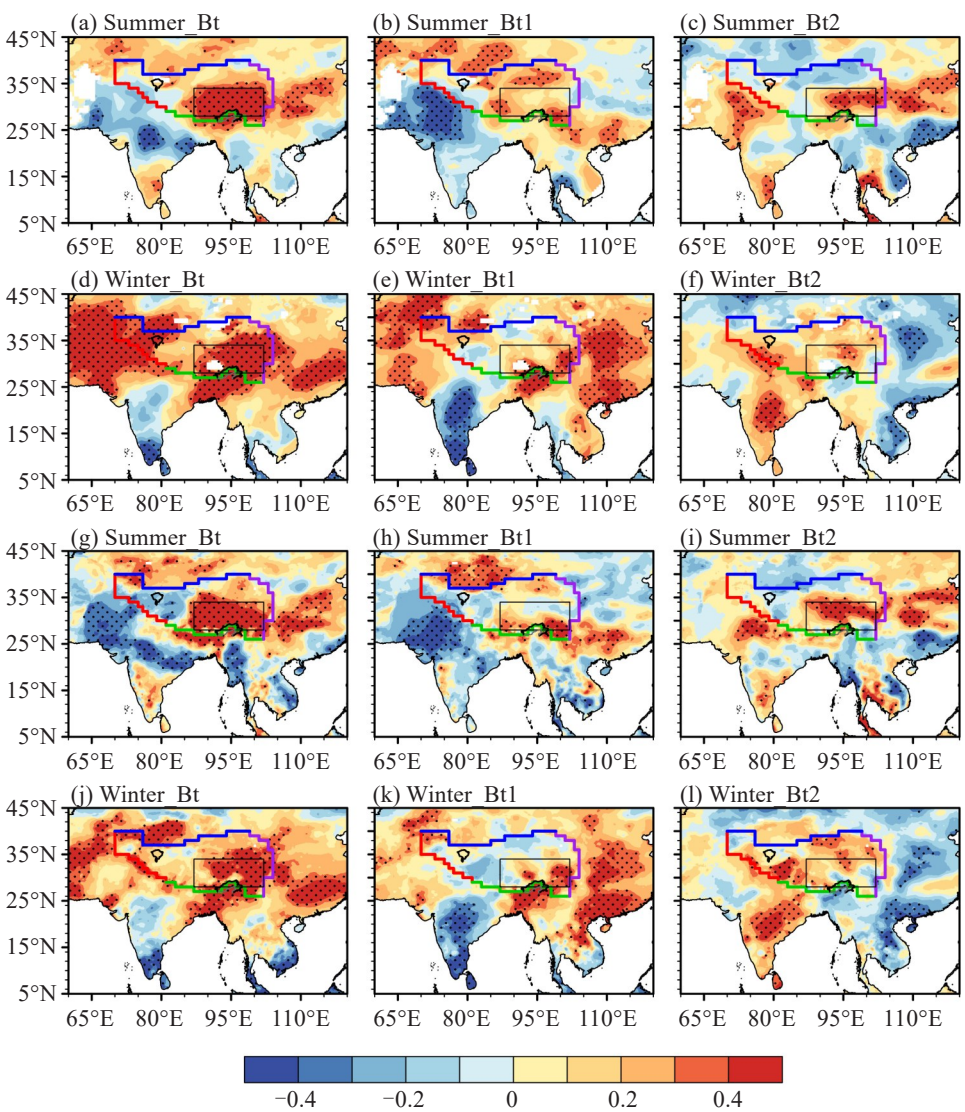

Figure 9. Spatial distributions of correlation coefficients between summer CRU precipitation and (a) the total water vapor budget (Bt), (b) the stationary water vapor budget (Bt1), (c) the transient water vapor budget (Bt2). (d)−(f) as in (a)−(c), but for winter CRU precipitation. (g)−(l) as in (a)−(f), but for APHRODITE precipitation. The dotted areas denote the correlation significant at the 90% confidence level. The linear trends of water vapor budget and precipitation have been removed. The black rectangle box denotes the CSETP region.

Table 4. Correlation coefficients of the CSETP precipitation index with Bt, Bt1, and Bt2 over the TP in summer and winter.

	Bt_summer	Bt1_ summer	Bt2_summer	Bt_winter	Bt1_ winter	Bt2_ winter
OBS	**0.77***	**0.30***	**0.30***	**0.69***	**0.32***	0.22
CRU	**0.72***	**0.28***	**0.28***	**0.65***	**0.32***	0.18
APHRODITE	**0.75***	0.21	**0.39***	**0.75***	**0.42***	0.08

Note: the linear trends of the variables were removed before the correlation coefficients were calculated. The differences indicated by an asterisk (*) are significant at the 90% confidence level.

5 CONCLUSIONS AND DISCUSSION

In this study, we systematically investigate the characteristics of the water vapor budget and the transient water vapor transport over the TP. The conclusions are summarized below.

(1) On the climatology, the TP is primarily controlled by the mid-latitude westerly-induced water vapor transport in spring and winter. The southwesterly-induced water vapor transport dominates the southern (southeastern) TP in summer (autumn). Moreover, water vapor from the South China Sea also contributes to autumn water vapor budget (Bt) over the TP. As a water vapor sink, the TP Bt is always positive in four seasons, peaking in summer (87×10^6 kg s^{-1}) and attaining its minimum value in winter (9×10^6 kg s^{-1}). The seasonal variation of Bt is typically determined by water vapor budget at the southern boundary (Bs) because of the counteraction between water vapor transport at the western and eastern boundaries. Furthermore, it should be noted that Bs is possibly overestimated with an ordinary rectangle boundary.

(2) The pattern in stationary water vapor transport resembles that in the total water vapor transport and reflects seasonal variation of the latter. The transient water vapor transport is mostly quasi-meridional in the mid- and high-latitude areas of Asia. The transient water vapor transport counteracts the stationary term at the northern boundary. For the climatological Bt over the TP, it is almost entirely contributed by the transient water vapor budget (Bt2) in winter. In the other seasons, however, the contribution of Bt2 to Bt is no more than one-fifth.

(3) The TP Bt shows a strong interannual variation and the associated water vapor transport pattern varies from season to season. On the whole, anomalous water vapor supplies from the Bay of Bengal, the North Arabian Sea, and mid-latitude West Asia through the western and southern boundaries regulate the annual variation of Bt. At the southern and western boundaries, Bt2 controls one-third to four-fifths of Bt anomalies.

(4) The TP Bt has a significantly positive connection with precipitation over the central-southern and southeastern parts of the TP in summer and winter, which is due to the joint regulation of Bt1 and Bt2. Taking the stationary and transient water vapor transports into account, the link between Bt and the CSETP precipitation is tighter and more credible. To sum up, the transient component could not be ignored when examining the interannual variation of the TP Bt and its impact on precipitation.

Due to the intense horizontal gradients in atmospheric water vapor content on the southern slope of the TP, summer Bs based on the irregular boundary along the topography may vary with the boundary location. That indicates differences of actual water vapor content over the TP at different elevations, which is important for the accurate estimation of water resources over the TP. In addition, an accurate description of the boundary cloud better realistically portray the relationship between the TP Bt and the loca precipitation relative to a rectangular boundary (figure omitted). Based on a relatively accurate boundary of the TP with an altitude above 2000 m, this study provides an insight into the transient water vapor transport and its contribution to the TP Bt. Due to the meridional direction of the transient water vapor transport, it could bring warm and wet water vapor from lower latitude inland or oceans and convey water vapor of the TP to the north, thus contributing to variations of Bt and precipitation over the TP. Compared with Bt1 which is calculated by the monthly mean data, Bt is closer with precipitation, especially in summer and winter. Further investigations may consider using multiple reanalysis datasets to better understand the effect of the transient water vapor transport.

In this study, it is seen that the TP Bt has a weaker connection with local precipitation in spring and autumn that in winter when there is which has less precipitation in a year. That may be related to the smaller spatial scale of anomalous water vapor transport associated with the TP Bt in spring and autumn (Figs. 6a and 6c). Xu et al. [47] also pointed out that regional precipitation is jointly affected by external water vapor transport, evapotranspiration, and local water vapor convergence and the leading factor may vary from season to season. The spring and autumn precipitation over the TP may also be susceptible to the other two factors except for water vapor transport. The specific impact factors of spring and autumn precipitation over the TP need to be further investigated.

Acknowledgments: The authors acknowledge the European Centre for Medium-Range Weather Forecasts (ECMWF) for providing ERA-Interim data (https://apps. ecmwf. int / datasets / data / interim-full-daily/), the China National Meteorological Information Center for providing the daily observational precipitation data (http://data.cma.cn/), the Asian Precipitation-Highly Resolved Observational Data Integration Towards the Evaluation of Water Resources (APHRODITE) for providing daily precipitation data (https://www. chikyu. ac. jp / precip / english / products. html), and the University of East Anglia Climatic Research Unit (CRU) for providing monthly precipitation data (https://crudata. uea. ac. uk / cru / data / hrg / cru_ts_4.05/cruts.2103051243.v4.05/pre/).

REFERENCE

[1] YAO T D, THOMPSON L, YANG W, et al. Different glacier status with atmospheric circulations in Tibetan Plateau and surroundings [J]. Nature Climate Change, 2012, 2(9): 663-667, https://doi.org/10.1038/nclimate1580

[2] XU X D, LU C G, SHI X H, et al. World water tower: An atmospheric perspective [J]. Geophysical Research Letters, 2008, 35(20): L20815, https://doi. org / 10.1029 / 2008gl035867

[3] MA Y Z, LU M Q, CHEN H N, et al. Atmospheric moisture transport versus precipitation across the Tibetan Plateau: A mini-review and current challenges [J]. Atmospheric Research, 2018, 209: 50-58, https://doi. org / 10.1016 / j. atmosres.2018.03.015

[4] IMMERZEEL W W, BEEK L P H V, BIERKENS M F P, et al. Climate change will affect the Asian water towers [J]. Science, 2010, 328(5984): 1382-1385, https://doi. org / 10.1126/science.1183188

[5] YAO T D, WU G J, XU B Q, et al. Asian water tower change and its impacts [J]. Bulletin of Chinese Academy of Sciences (in Chinese), 2019, 34(11): 1203-1209, http://dx. doi.org/10.16418/j.issn.1000-3045.2019.11.003

[6] ZHAO P, XU X D, CHEN F, et al. The third atmospheric scientific experiment for understanding the earth-atmosphere coupled system over the Tibetan Plateau and its effect [J]. Bulletin of the American Meteorological Society, 2018, 99(4): 757-776, https://doi. org / 10.1175 / bams-d-16-0050.1

[7] ZHOU T J, GAO J, ZHAO Y, et al. Water vapor transport processes on Asian water tower [J]. Bulletin of Chinese Academy of Sciences (in Chinese), 2019, 34(11): 1210-1219, http://dx. doi. org / 10.16418 / j. issn. 1000-3045.2019.11.004

[8] YE D Z, GAO Y X. Meteorology of the Qinghai-Xizang Plateau [M]. Beijing: Science Press, 1979 (in Chinese).

[9] YAO T D, MASSON - DELMOTTE V, GAO J, et al. A review of climatic controls on $\delta^{18}O$ in precipitation over the Tibetan Plateau: Observations and simulations [J]. Reviews of Geophysics, 2013, 51(4): 525-548, http://dx. doi. org / 10.1002/rog.20023

[10] CURIO J, MAUSSION F, SCHERER D. A 12-year high-resolution climatology of atmospheric water transport over the Tibetan Plateau [J]. Earth System Dynamics, 2015, 6(1): 109-124, https://doi. org / 10.5194 / esd-6-109-2015

[11] WANG Z Q, DUAN A M, YANG S, et al. Atmospheric moisture budget and its regulation on the variability of summer precipitation over the Tibetan Plateau [J]. Journal of Geophysical Research: Atmospheres, 2017, 122(2): 614-630, https://doi.org/10.1002/2016jd025515

[12] ZHANG C, TANG Q H, CHEN D L. Recent changes in the moisture source of precipitation over the Tibetan Plateau [J]. Journal of Climate, 2017, 30(5): 1807-1819, https://doi.org/10.1175/jcli-d-15-0842.1

[13] SUGIMOTO S, UENO K, SHA W M. Transportation of water vapor into the Tibetan Plateau in the case of a passing synoptic-scale trough [J]. Journal of the Meteorological Society of Japan, 2008, 86(6): 935-949, https://doi.org/10.2151/jmsj.86.935

[14] SHI X Y, SHI X H. Climatological characteristics of summertime moisture budget over the southeast part of Tibetan Plateau with their impacts [J]. Journal of Applied Meteorological Science (in Chinese), 2008, 19(1): 41-46.

[15] BOTHE O, FRAEDRICH K, ZHU X H, et al. The large-scale circulations and summer drought and wetness on the Tibetan Plateau [J]. International Journal of Climatology, 2009, 30(6): 844-855, https://doi.org/10.1002/joc.1946

[16] GAO Y H, CUO L, ZHANG Y X. Changes in moisture flux over the Tibetan Plateau during 1979-2011 and possible mechanisms [J]. Journal of Climate, 2014, 27(5): 1876-1893, https://doi.org/10.1175/JCLID-13-00321.1

[17] ZHOU C Y, LI Y Q, LI W, et al. Climatological characteristics of water vapor transport over eastern part of Qinghai-Xizang Plateau and its surroundings [J]. Plateau Meteorology (in Chinese), 2005, 24(6): 880-888

[18] FENG L, ZHOU T J. Water vapor transport for summer precipitation over the Tibetan Plateau: Multidata set analysis [J]. Journal of Geophysical Research: Atmospheres, 2012, 117: D20114, https://doi.org/10.1029/2011jd017012

[19] MENG D L, DONG Q, KONG F P, et al. Spatio-temporal variations of water vapor budget over the Tibetan Plateau in summer and its relationship with the Indo-Pacific warm Pool [J]. Atmosphere, 2020, 11(8): 828, https://doi.org/10.3390/atmos11080828

[20] GAO D Y, ZOU H, WANG W. Influence of water vapor channels of Brahmaputra on precipitation [J]. Mountain Research (in Chinese), 1985, 3(4): 239-249.

[21] XU X D, TAO S Y, WANG J Z, et al. The relationship between water vapor transport features of Tibetan Plateau-Monsoon "large triangle" affecting region and drought-flood abnormality of China [J]. Acta Meteorological Sinica (in Chinese), 2002, 60(3): 257-267.

[22] ZHOU C Y, ZHAO P, CHEN J M. The interdecadal change of summer water vapor over the Tibetan Plateau and associated mechanisms [J]. Journal of Climate, 2019, 32(13): 4103-4119, https://doi. org / 10.1175 / jcli-d-18-0364.1

[23] LIU X D, YIN Z Y. Spatial and temporal variation of summer precipitation over the Eastern Tibetan Plateau and the North Atlantic Oscillation [J]. Journal of Climate, 2001, 14(13): 2896-2909, https://doi. org / 10.1175 / 1520-0442(2001)014<2896:SATVOS>2.0.CO;2

[24] GAO Y, WANG H J, LI S L. Influences of the Atlantic Ocean on the summer precipitation of the southeastern Tibetan Plateau [J]. Journal of Geophysical Research: Atmospheres, 2013, 118(9): 3534-3544, https://doi. org / 10.1002/jgrd.50290

[25] DONG W H, LIN Y L, WRIGHT J S, et al. Summer rainfall over the southwestern Tibetan Plateau controlled

by deep convection over the Indian subcontinent [J]. Nature Communications, 2016, 7: 10925, https://doi.org/10.1038/ncomms10925

[26] JIANG X W, TING M F. A dipole pattern of summertime rainfall across the Indian subcontinent and the Tibetan Plateau [J]. Journal of Climate, 2017, 30(23): 9607-9620, https://doi.org/10.1175/jcli-d-16-0914.1

[27] CHEN B, ZHANG W, YANG S, et al. Identifying and contrasting the sources of the water vapor reaching the subregions of the Tibetan Plateau during the wet season [J]. Climate Dynamics, 2019, 53(11): 6891-6907, https://doi.org/10.1007/s00382-019-04963-2

[28] YAN H R, HUANG J P, HE Y L, et al. Atmospheric water vapor budget and its long-term trend over the Tibetan Plateau [J]. Journal of Geophysical Research: Atmospheres, 2020, 125(23): e2020JD033297, https://doi.org/10.1029/2020jd033297

[29] LIU X L, LIU Y M, WANG X C, et al. Large-scale dynamics and moisture sources of the precipitation over the western Tibetan Plateau in boreal winter [J]. Journal of Geophysical Research: Atmospheres, 2020, 125(9): e2019JD032133, https://doi.org/10.1029/2019JD032133

[30] LIU Y, CHEN H P, LI H, et al. What induces the interdecadal shift of the dipole patterns of summer precipitation trends over the Tibetan Plateau? [J]. International Journal of Climatology, 2021, 41(11): 5159-5177, https://doi.org/10.1002/joc.7122

[31] HU S, ZHOU T J, WU B. Impact of developing ENSO on Tibetan Plateau summer rainfall [J]. Journal of Climate, 2021, 34(9): 3385-3400, https://doi.org/10.1175/JCLI-D-20-0612.1

[32] XIE C Y, LI M J, ZHANG X Q. Characteristics of summer atmospheric water resources and its causes over the Tibetan Plateau in recent 30 years [J]. Journal of Natural Resources (in Chinese), 2014, 29(6): 979-989.

[33] LU N, QIN J, GAO Y, et al. Trends and variability in atmospheric precipitable water over the Tibetan Plateau for 2000-2010 [J]. International Journal of Climatology, 2015, 35(7): 1394-1404, https://doi.org/10.1002/joc.4064

[34] LU N, TRENBERTH K E, QIN J, et al. Detecting long-term trends in precipitable water over the Tibetan Plateau by synthesis of station and MODIS observations [J]. Journal of Climate, 2015, 28(4): 1707-1722, https://doi.org/10.1175/JCLI-D-14-00303.1

[35] YI L, TAO S Y. Role of the standing and the transient eddies in atmospheric water cycle in the Asian monsoon region [J]. Acta Meteorological Sinica (in Chinese), 1997, 55(5): 532-544.

[36] ZHOU T J, ZHANG X H, WANG S W. The air-sea freshwater exchange derived from NCEP / NCAR reanalysis data [J]. Acta Meteorological Sinica (in Chinese), 1999, 57(3): 264-282.

[37] LIU G W, CUI Y F. The eddy transport of atmospheric moisture over China [J]. Advances in Water Science (in Chinese), 1991, 2(3): 145-153.

[38] PIAO J L, CHEN W, ZHANG Q, et al. Comparison of moisture transport between Siberia and northeast Asia on annual and interannual time scales [J]. Journal of Climate, 2018, 31(18): 7645-7660, https://doi.org/10.1175/jcli-d-17-0763.1

[39] DEE D P, UPPALA S M, SIMMONS A J, et al. The ERA-Interim reanalysis: configuration and performance of the data assimilation system [J]. Quarterly Journal of the Royal Meteorological Society, 2011, 137(656): 553-597, https://doi.org/10.1002/qj.828

[40] YATAGAI A, ARAKAWA O, KAMIGUCHI K, et al. A 44-year daily gridded precipitation dataset for Asia based on a dense network of rain gauges [J]. Sola, 2009, 5: 137-140, https://doi.org/10.2151/sola.2009-035

[41] HARRIS I, OSBORN T J, JONES P, et al. Version 4 of the CRU TS monthly high-resolution gridded multivariate climate dataset [J]. Scientific Data, 2020, 7: 109, https://doi.org/10.1038/s41597-020-0453-3

[42] WANG B Y, FAN G Z, ZHOU D W. Characteristics of moisture transport in summer over the Tibetan Plateau [J]. Resources and Environment in the Yangtze Basin (in Chinese), 2014, 23(Z1): 979-989.

[43] LI Y T, ZHAO L N, GONG Y F, et al. The relationship and formation of springtime southern branch trough and precipitation in China [J]. Journal of Chengdu University of Information Technology (in Chinese), 2017, 32(3): 282-288.

[44] JIANG W X, JIA L, XIAO T G. Study of spatial and temporal characteristics on winter precipitation in the Tibetan Plateau [J]. Journal of Chengdu University of Information Technology (in Chinese), 2014, 29(6): 644-651.

[45] HU L, LI Y D, FU R, et al. The relationship between mobile mesoscale convective systems over the Tibetan Plateau and the rainfall over eastern China in summer [J]. Plateau Meteorology (in Chinese), 2008, 27(2): 301-309.

[46] ZHAO Y, CHEN D L, DENG Y, et al. How were the eastward-moving heavy rainfall events from the Tibetan Plateau to the lower reaches of the Yangtze River enhanced? [J]. Journal of Climate, 2021, 34(2): 607-620, https://doi.org/10.1175/jcli-d-20-0226.1

[47] XU D, KONG Y, WANG C H. Change of water vapor budget in arid area of northwest China and its relationship with precipitation [J]. Journal of Arid Meteorology (in Chinese), 2016, 34(3): 431-439.

Citation: WANG Hui-mei, ZHAO Ping. Spatiotemporal Variation of Water Vapor Budget over the Tibetan Plateau and Its Regulation on Precipitation [J]. Journal of Tropical Meteorology, 2022, 28(2): 194-206, https://doi. org / 10.46267 / j. 1006-8775.2022.015